

Chapter 6

Mechanism of Py-Im Polyamide-Induced Cytotoxicity in Prostate Cancer Cells

John W. Phillips, Benjamin C. Li, Kenneth K. Karanja, Judith L. Campbell, and
Peter B. Dervan.

Manuscript in preparation.

Abstract

We have developed 8-ring, hairpin, Py-Im polyamides that downregulate the expression of Androgen Receptor (AR) target genes in LNCaP cells. These compounds are cell-permeable, sequence-specific, high-affinity DNA minor groove binders that are designed to prefer the sequence 5'-WGWWCW-3' (W=A or T). This study investigates the cytotoxicity of polyamides targeted to this sequence in prostate cancer cells. We determine that these compounds are cytotoxic at micromolar concentrations and that this property is not dependent on intact AR signaling. Polyamide-treated cells undergo apoptotic cell death as marked by Caspase 3/7 activation and PARP cleavage after 24 hours. Prior to inducing programmed cell death, polyamide-treated cells arrest in S-phase. S-phase arrest occurs despite the apparent absence of DNA damage and without activating the DNA damage-induced S-phase checkpoint. The cytotoxic effects and cell cycle disruption produced by the AR-targeted polyamides in prostate cancer cells suggest that inhibition of AR-driven gene expression with these compounds is accompanied by AR-independent cell death.

6.1. Introduction

Py-Im polyamides are programmable small molecules capable of binding to DNA with affinities and specificities comparable to DNA-binding proteins (1). The sequence specificity arises from pairs of *N*-methylpyrrole (Py) and *N*-methylimidazole (Im) amino acids that interact with the hydrogen bonding pattern produced by DNA base pairs in the minor groove: Im/Py specifies a G-C base pair, Py/Im a C-G base pair, and Py/Py specifies T-A or A-T (2). They are cell-permeable compounds that localize to the nucleus in live cells and bind genomic DNA in its chromatin form (3-7). When designed to bind DNA sequences that match the response element of an endogenous transcription factor, they can disrupt the transcription factor-DNA interface and selectively inhibit inducible changes in downstream target gene expression (8-11). The Py-Im polyamide represents a framework for the development of chemical tools to control gene expression.

We have developed a polyamide (1) that antagonizes steroid-induced gene expression changes driven by the nuclear hormone receptors androgen receptor (AR) and glucocorticoid receptor (GR) (Figure 6.1). In animals, these transcription factors form powerful nodes in the transduction of signals from circulating hormones: AR controls the development and maintenance of the male sexual phenotype in response to testosterone, and GR regulates the expression of anti-inflammatory genes in response to

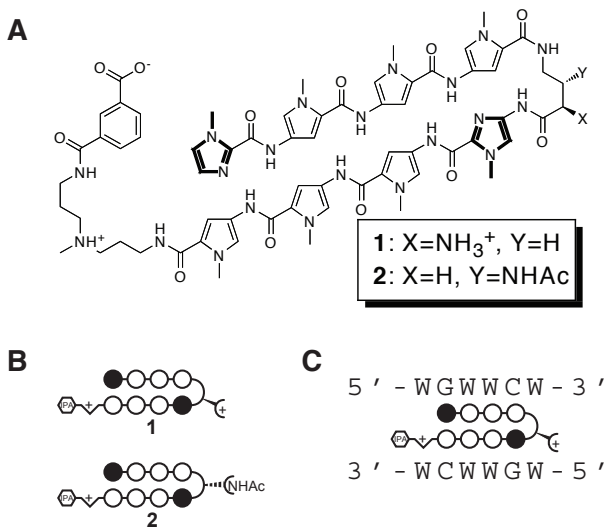


Figure 6.1. Chemical structure and binding preferences of the Py-Im polyamides used in this study. (A) Chemical structure showing the two different turn functionalities (B) Ball-and-stick representation of the polyamides. Open circles represent *N*-methylpyrrole residues, filled circles represent *N*-methylimidazoles. The hexagon represents the isophthalic acid moiety. (C) Both 1 and 2 bind the same 5'-WGWWCW-3' DNA sequence, where W = A or T.

cortisol (12,13). In the absence of ligand, nuclear hormone receptors are sequestered in the cytosol by heat shock proteins (HSPs). Steroid binding causes an allosteric conformational shift followed by homodimerization, nuclear localization, response element binding, and modulation of target gene transcription (14). AR and GR share the consensus binding sequence 5'-GGTACANNNTGTTCT-3' (15). Their genotropic actions can be partially inhibited in cancer tissue culture cells by polyamide **1**, which disrupts the protein-DNA interface by selectively binding the DNA sequence 5'-WGWWCW-3' (W= A or T) (8,10). In prostate cancer cells, AR signaling is mitogenic; whether or not this part of the androgen axis is inhibited by ARE-targeted polyamides is one of the subjects of this study.

Polyamides may be specific inhibitors of transcription factor-DNA binding in cell culture, but they are also part of a larger class of non-covalent, DNA-minor groove binders. This class of compounds includes the natural products distamycin A and netropsin as well as synthetic compounds like Hoechst 33342 and pentamidine (16). Of all of these, distamycin is perhaps the best studied. This compound binds to DNA with 2:1 stoichiometry and high affinity ($K_a \approx 3 \times 10^8$), and is selective for A-T tracts (17-19). In cell culture, distamycin is known to inhibit the activity of topoisomerases I and II and to interfere with gene regulation by disrupting the binding of high mobility group (HMG) domain-containing proteins to DNA (20,21). *In vitro*, it is known to inhibit the activity of RNA and DNA polymerases as well as WRN and BLM helicases (22,23). Its cytotoxicity is in the 400 μ M range, and it is unknown which of these processes induces cell death. Derivatives appended with alkylating or other adduct-forming functionalities are two to three orders of magnitude more potent (24).

This study addresses the growth-inhibitory and cytotoxic properties of two structurally related Py-Im polyamides (compounds **1** and **2**, Figure 6.1). They are selective for the same 5'-WGWWCW-3' DNA sequence, and both downregulate the expression of AR target genes in LNCaP cell culture, albeit with different potencies (25). To explore the AR dependence of any potential growth inhibitory effects, we establish the cytotoxicity

of these compounds in cell culture models of hormone-sensitive and hormone-refractory prostate cancer. Using assays for Caspase 3/7 activity and PARP cleavage, we show the cell death to be apoptotic in nature. Flow cytometric cell cycle analysis reveals a dose-dependent S-phase arrest. S-phase stress is often the result of DNA damage, but single cell alkaline gel electrophoresis and Western blot analysis of checkpoint proteins show no evidence of single- or double-strand DNA breaks. The results have important implications for the design and use of Py-Im polyamides as chemical probes of protein-DNA interactions in biological systems.

6.2. Results.

6.2.1. Cytotoxicity of a Py-Im polyamide in prostate cancer cells. We conducted cytotoxicity assays with compounds **1** and **2** in three different prostate cancer cell lines. LNCaP is a tissue culture model of hormone-sensitive prostate cancer (26). LNAR is an engineered LNCaP cell line containing a stably incorporated construct that increases AR expression roughly 5-fold (27). In tumor xenograft studies in mice, this upregulation was sufficient to induce resistance to first-generation anti-androgens. The third cell line, DU145, expresses very low levels of AR and does not produce PSA or exhibit androgen-dependent growth: it is considered hormone insensitive (28). The compounds displayed time- and dose-dependent cytotoxicity at 72 and 96 h as measured by sulfarhodamine B staining in all three cell lines, regardless of AR status (Table 6.1). There was no correlation between AR status and IC_{50} value, suggesting

that the observed cytotoxicity occurred via an AR-independent mechanism. Compound **2** had approximately tenfold higher

potency than compound **1** at both time points, which is consistent with its previously reported increased potency

against AR-driven gene expression. This may represent uptake differences between the two compounds, as small structural changes have been observed to dramatically change the cellular uptake properties of polyamides (29).



Cell line	AR	Cytotoxicity IC_{50} values (μ M)			
		 1		 2	
		72h	96h	72h	96h
LNCaP	+	18±4	7±3	1.8±0.9	0.6±0.2
LNAR	+++	40±10	36±14	3±1	1.5±0.2
DU145	-	14±4	8±4	1.5±0.5	0.76±0.06

Table 6.1. Summary of cytotoxicity IC_{50} values of WG-WWCW-targeted polyamides in AR-expressing (+, LNCaP), AR-overexpressing (+++, LNAR), and AR-negative (-, DU145) cancer cell lines. Cells were treated continuously with test compounds for 72 or 96 h. before fixation and staining. Values represent the mean \pm s.d. of three replicates.

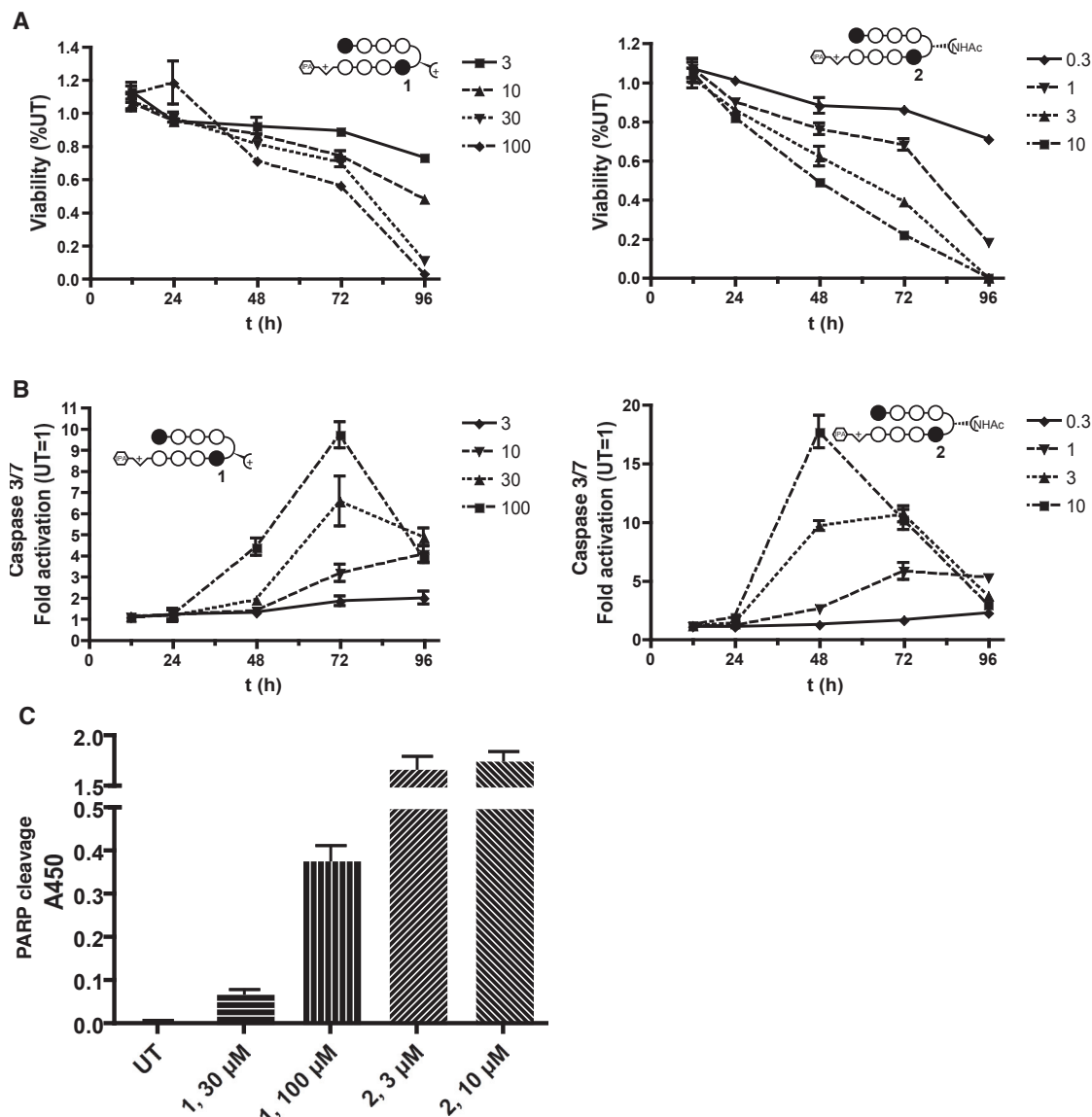


Figure 6.2. Polyamide treatment induces apoptosis in DU145 cells. (A) Cell viability assay. Cells were treated in quadruplicate with a range of polyamide concentrations for up to 96 h and then assayed for bioreductive capacity with WST-1 reagent. The data are normalized to the untreated condition. (B) Caspase 3/7 activity assay. Cells were treated in triplicate for the indicated time and then homogenized in guanidinium lysis buffer containing a proluminescent Caspase 3/7 substrate. The data are normalized to the untreated condition. (C) ELISA for cleaved PARP formation. Cells were treated with compounds for 72 h before assaying the lysates by sandwich ELISA using an HRP-conjugated secondary antibody and a chromogenic substrate. The data are presented as the background-corrected absorbance values at 450 nm. All data are represented as the mean \pm s.d. of experiments conducted in triplicate or quadruplicate.

binding agents involves induction of apoptosis, two hallmarks of which are caspase activation and subsequent cleavage of poly(ADP-ribosyl) transferase (PARP) (30). To assess the involvement of the apoptotic pathway in the cell death response to polyamide treatment, we treated DU145 cells with the polyamides and assayed for decreased cell viability and

Caspase 3/7 over the same time course (Figure 6.2). Viability was measured with WST-1 reduction; Caspase 3/7 activation was measured with a proluminescent peptide substrate. Steep declines in viability did not occur until after 48 h of treatment with polyamide **1** or 72 h. of treatment with compound **2**. Cell viability decreased concomitantly with induction of Caspase 3/7 activity in a time- and concentration-dependent manner. With compound **1**, elevated levels of Caspase 3/7 activity were detected over the entire dose range (3-100 μ M), with peak activity measured at approximately tenfold activation with 100 μ M **1** after 72 h. The results were similar with **2**, albeit with earlier caspase induction at approximately ten-fold lower concentration than was observed with **1**. Caspase activation was also accompanied by PARP cleavage, as measured after 72 h. continuous exposure by sandwich ELISA (Figure 6.2C), confirming that the cell death response to polyamide treatment involves apoptosis.

6.2.3. Polyamide treatment induces replication stress. Many DNA-binding agents are known to cause cell cycle disturbances. To examine the effects of polyamides **1** and **2** on the cell cycle, we pulse-labeled polyamide-treated DU145 cells for 30 min. with ethynyldeoxyuridine (EdU) after 24 h of compound treatment at various concentrations (Figure 6.3). The cells were harvested, and the incorporated, EdU-labeled nucleotides were conjugated with an azido-Alexa488 fluorophore using copper-catalyzed cycloaddition chemistry. Total DNA content was determined with 7-aminoactinomycin D staining, and the cells were subjected to two-color flow cytometric analysis. Both compounds produced a dose-dependent increase in the percentage of cells in S-phase, with a corresponding drop in the percentage of G_0/G_1 cells. The proportion of G_2/M phase cells was not affected in a dose-dependent fashion. In addition, although the percentage of cells in S-phase increased, the average intensity of EdU staining decreased, suggesting that the treated cells were replicating their DNA more slowly.

6.2.4. Polyamide treatment does not cause DNA damage.

S-phase arrest subsequent to treatment with a DNA binding compound is suggestive of S-phase checkpoint activation in response to DNA damage or replication stress. In this pathway, DNA lesions and stalled replication forks activate ATM/ATR kinases. These proteins phosphorylate many substrates to activate checkpoints that slow cell cycle progression and allow time for DNA damage repair (31). In the presence of DNA damage, ATR phosphorylates RPA2 at S4 and S8, and CHK1 at S345 (32,33). ATM phosphorylates CHK2 at T68 after DNA damage by ionizing radiation. However, CHK2 is also phosphorylated in an ATM-independent manner after replication stress caused by depletion of nucleotide pools by hydroxyurea (34,35).

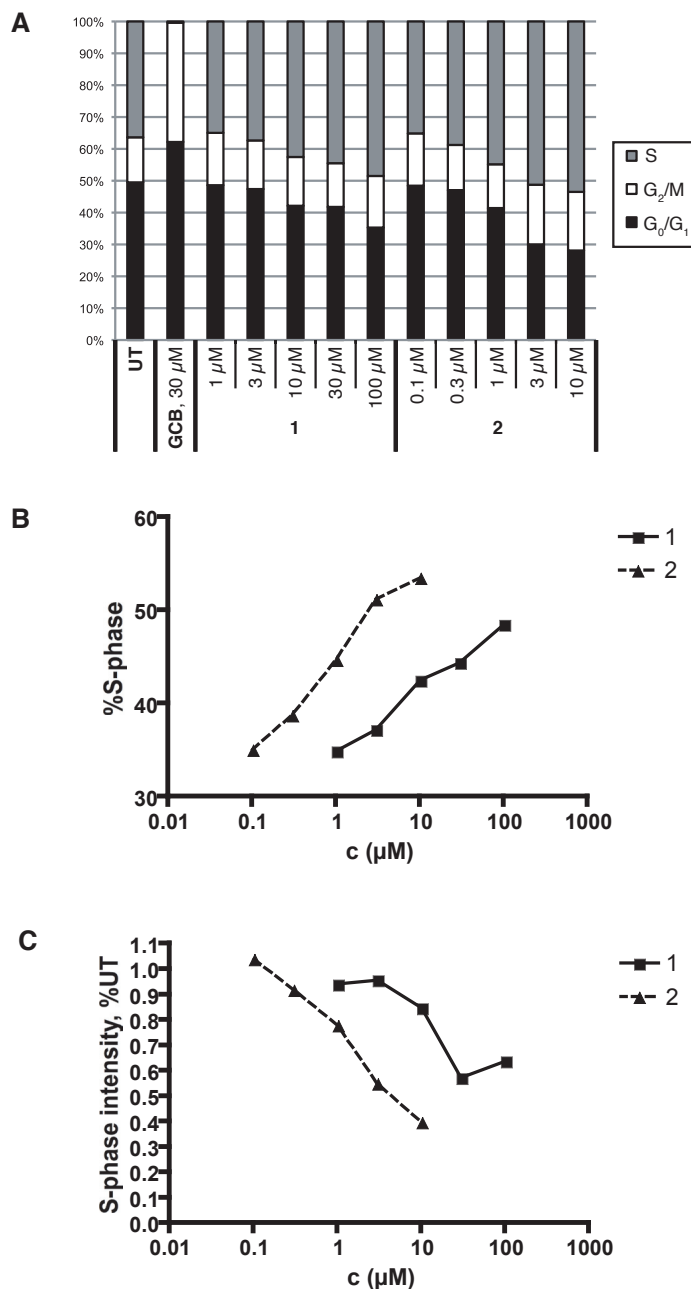


Figure 6.3. Polyamide treatment causes S-phase arrest. (A) Cell cycle distribution of DU145 cells treated with compounds or controls for 24h as measured by two-color flow cytometric evaluation of EdU pulse-labeled cells stained for DNA content with 7AAD. (B) %S-phase data from (A) shown as a function of increasing polyamide dose showing S-phase arrest. (C) Dose-dependent decrease in average EdU incorporation indicative of slowed DNA synthesis in response to polyamide treatment. 20,000 cells were counted for each sample. The experiment was conducted in duplicate.

To look for activation of the S-phase checkpoint by DNA damage or replication stress, we treated DU145 cells with toxic levels of compounds **1** and **2** (30 and 3 μM , respectively) for 18 h and then performed Western blotting on total cellular lysates using phospho-specific antibodies against RPA2, CHK1, and CHK2 (Figure 6.4A). Etoposide, a DNA-binding compound that poisons Topoisomerase II (TOPII) to produce DNA double-strand breaks, was included as a positive control. In the polyamide-treated samples, none of the markers of DNA damage during S-phase were activated; no phospho-CHK1, -CHK2, or -RPA2 was detected.

The absence of downstream signals from ATM/ATR suggests that the S-phase arrest seen in polyamide-treated cells is not due to DNA damage from stalled replication forks. Histone H2AX, a marker of DNA double-strand breaks (36), was observed to be phosphorylated when the cells were treated with 10 μM **2**. Although ATM rapidly phosphorylates H2AX in response to DNA damage, the absence of any other signals of DNA damage suggests

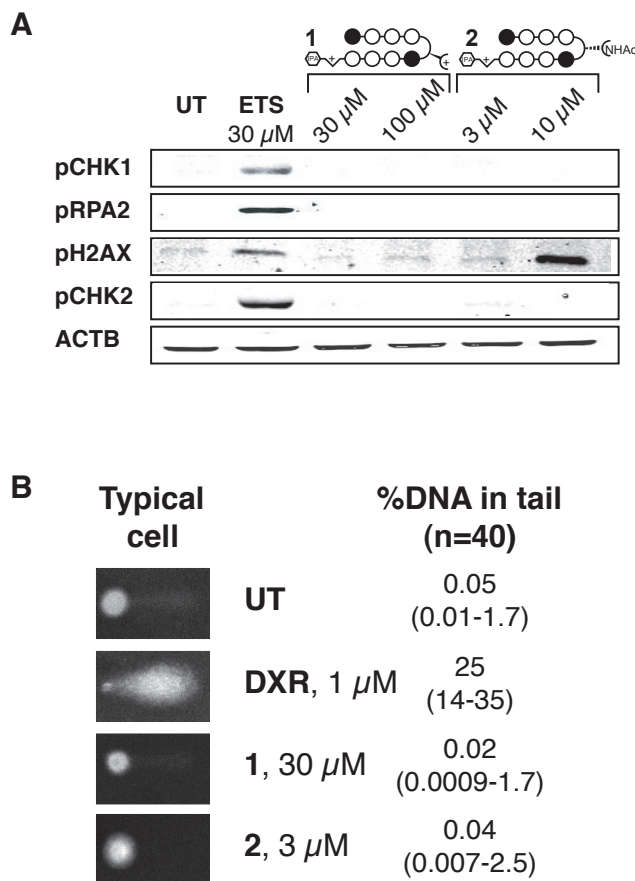


Figure 6.4: Polyamide treatment does not induce DNA damage or activate the DNA-damage induced S-phase checkpoint. (A) Western blot of S-phase and DNA damage response proteins using phospho-specific antibodies to probe DU145 lysates from cells treated with polyamides or controls for 18 h. (B) Single cell gel electrophoretic analysis of DU145 cells treated with polyamides or controls for 24 h. Photomicrographs of a representative cell nucleus from each treatment condition are shown on the left. Migration of DNA from the centroid is proportional to the amount of DNA damage. Images of 40 randomly selected cells from each treatment condition were analyzed with image processing software to determine the percentage of DNA in each 'tail.' The data are expressed as the median and 95% confidence values.

an alternative, independent mechanism for its phosphorylation in this case. Namely, the observed phospho-H2AX at high concentrations of **2** may be a result of apoptotic activation of caspase cleavage of DNA.

To look for DNA damage as a result of polyamide treatment more directly, we subjected DU145 cells to cytotoxic levels of the two polyamides for 24 h and then assayed them by semiquantitative single cell alkaline gel electrophoresis (comet assay) (Figure 6.4B). Migration of the DNA from the centroid into the 'comet tail' is proportional to the amount of single- and double-strand breakage that has occurred. Cells treated with doxorubicin, a known DNA-damaging agent, had a median value of 25% of total DNA in the tail. Polyamide-treated cells were indistinguishable from the untreated control, with median tail % values of 0.02 and 0.04 for compounds **1** and **2**, respectively.

6.3. Discussion

This study seeks to define the effects of two 8-ring, hairpin, Py-Im polyamide antagonists of AR-driven gene expression on the growth and viability of prostate cancer cells. We show that polyamides **1** and **2** cause cytotoxic effects and cell cycle disturbance at concentrations known to interfere with the induction of some AR-target genes in LNCaP cells in response to androgen stimulus (10,25). AR signaling is mitogenic in LNCaP cells, but the set of the genes involved is still being defined with massively parallel sequencing techniques (37). Nevertheless, anti-androgen steroid antagonists like bicalutamide slow the growth of this cell line, producing arrest in the G_0/G_1 phase of the cell cycle and apoptosis (38,39). The mechanism of cell death produced by AR-targeted polyamides also involves apoptosis, but there is no dependence on intact AR signaling to produce this effect; the polyamides are equitoxic in LNCaP (AR+, hormone-sensitive) and DU145 (AR-, hormone-insensitive) cells. In addition, the growth arrest due to polyamide treatment occurs in S-phase, not in G_0/G_1 . The polyamide AR antagonists retard the growth of cancer cells independent of their effects on AR-regulated mRNA expression.

The cytotoxic effects of the polyamides used in this study are observed in the same concentration range and on the same timescale as their effects on AR-driven gene expression. These data suggest that it may not be possible to divorce their specific effects on AR-ARE binding from their non-AR-related induction of programmed cell death based on dose titration. Compounds **1** and **2** both bind the DNA sequence 5'-WGWWCW-3', a relatively short and degenerate motif that occurs millions of times in the human genome. The AR consensus DNA binding sequence is also degenerate, but transcription factors can take advantage of a wealth of additional interactions including protein-protein contacts and allosteric modulation of the DNA topology to restrict their binding to a defined set of response elements (40). Future efforts to disrupt transcription factor-DNA binding with polyamides may need to focus on compounds with higher specificity. For example,

polyamides with higher imidazole content would have fewer binding sites genome wide, as would larger compounds with 10 or 12 ring pairs that could specify 8 or 10 DNA base pairs. In fact, larger hairpin compounds containing beta-alanine residues to increase flexibility have been employed to inhibit the binding of the AP-1 transcription factor in order to downregulate MMP9 expression in cell culture and mouse models of metastatic colorectal cancer (41).

The S-phase growth arrest produced by polyamides **1** and **2** may be the signal event that produces the eventual cytotoxicity. The effects on the cell cycle are large and occur in advance of the drop in cell viability. S-phase arrest is apparent after 18 h of continuous treatment, whereas the cell viability does not drop sharply until at least 24 h of treatment (Figure 6.2). In addition to the temporal considerations, one should note that the 10-fold difference in potency between the two compounds in the cytotoxicity assay is also present in the cell cycle data. Compound **2** produces cell cycle disturbance at 10-fold lower concentrations than compound **1**. Compound **2** also produces a greater maximal inhibition of EdU incorporation than compound **1**. The size of the cell cycle disturbance, its relatively rapid onset, and its correlation with the cytotoxicity IC_{50} values suggest that inhibition of DNA synthesis is a primary mechanism of polyamide-induced cytotoxicity.

The fact that the accumulation of cells in S-phase produced by the polyamides occurs in the absence of any observable DNA damage suggests activation of a damage-independent intra-S phase checkpoint. The absence of CHK1, RPA2 and H2AX phosphorylation tends to rule out DNA damage, while the absence of CHK2 phosphorylation suggests that although replication is impeded, the replication forks have not collapsed to form double stranded breaks. Activation of the intra-S phase checkpoint can arise after phosphorylation of the replisome proteins including MCM2-7, MCM10 and DNA polymerases (42). In metazoans, conditions of replicative stress or DNA damage led to phosphorylation of MCM2-7, the replicative helicase, by ATM/ATR to activate a checkpoint (43-45). Examining other substrates of ATM/ATR phosphorylated after replicative stress could help

define the mechanism of polyamide-induced S-phase arrest.

One possibility is that the polyamides are interfering with replication by inhibiting topoisomerase function. But as non-covalent minor groove binders, polyamides would be anticipated to inhibit binding of these enzymes to DNA without causing formation of the cleavable complex required to generate DNA damage. In addition, inhibitors of TOPI or TOPII catalytic activity arrest cells in G2/M due to activation of the G2/M checkpoint or decatenation failure (46,47), not in S-phase as observed. An additional possibility is that the polyamides are inhibiting replicative DNA helicase activity, as the structurally related DNA minor groove-binder distamycin is known to do *in vitro*. However, it is unclear if this mode of inhibition would be expected to produce DNA damage, for a synthetic WRN helicase inhibitor was recently shown to cause S-phase delay and H2AX phosphorylation in cell culture (48). Studies of fork progression using *in vitro* reconstitution models would be useful for defining the biochemical target for polyamide cytotoxicity.

6.4. Materials and methods

6.4.1. Chemicals and reagents. Compounds **1** and **2** were synthesized on solid phase Kaiser oxime resin using previously published protocols (49). Cell culture media was purchased from Invitrogen, and fetal bovine serum from Irvine Scientific. Gemcitabine was purchased from AvaScientific. Etoposide and doxorubicin were purchased from Sigma-Aldrich, as were all other reagents unless otherwise noted.

6.4.2. Cell culture. LNCaP, LNAR, and DU145 cells were maintained in RPMI 1640 with 10% FBS at 37 °C under 5% CO₂. LNCaP and DU145 cells were purchased from ATCC (Manassas, VA). LNAR cells were a gift from C.L. Sawyers at Memorial Sloan-Kettering Cancer Center (NY, NY).

6.4.3. Cytotoxicity assays. IC₅₀ values for cytotoxicity were determined using a previously-described, sulfarhodamine-based, colorimetric assay for cellular protein content in 96-well microplates (50). LNCaP and LNAR cells were plated at 3,000 or 4,000 cells per well for the 72 h and 96 h timepoints, respectively. DU145 cells were plated at 2,000 or 2,500 cells per well. Compounds were added in 100 μL RPMI1640 supplemented with 10% FBS 24 h after plating. Quadruplicate wells were used for each concentration. At the appropriate time, the cells were fixed with 100 μL 10% trichloroacetic acid solution, washed, stained, and dried as described. After solubilization of the bound dye in 10 mM Tris (pH 8), the absorbance was measured at 490 nm on a Victor microplate reader (PerkinElmer).

The data are charted as a percentage of untreated controls, corrected for background absorbance. IC₅₀ is defined as the concentration that inhibits 50% of control cell growth. These values were determined by non-linear least-squares regression fit to $Y = A + (B - A) / (1 + 10^{((\text{Log EC}_{50} - X) * H)})$, where A=max., B=min., and H=Hill Slope. Three independent trials were averaged; stated IC₅₀ values represent the mean and standard deviation. These

calculations were performed using Prism 4 (GraphPad) software.

6.4.4. Apoptosis assays. DU145 cells were plated in 96-well microplates at 2,000-8,000 cells per well. As above, compounds and controls were added 24 h after plating. Each time point was assayed in triplicate. At harvest, Caspase 3/7 activity was assessed using 100 μ L of Caspase-Glo reagent (Promega), which contains the proluminescent caspase substrate DEVD-aminoluciferin. Luminescence was measured after 30 min incubation at room temperature. Luminescence data are expressed as a fold difference from untreated controls as measured using a Victor microplate reader (PerkinElmer).

The cell viability of each treatment condition was monitored in a sister plate using a tetrazolium-based assay for mitochondrial bioreductive capacity (51). 10 μ L WST-1 reagent (Roche) was added to each well and incubated at 37 °C for 30 min before measuring the absorbance at 450 nm. The WST-1 data are corrected for background absorbance and expressed as a percentage of untreated controls.

6.4.5. PARP cleavage assay. 400,000 DU145 cells were plated in 10 cm diameter dishes. Compounds were added after 24 h and were allowed to incubate an additional 72 h. At harvest, cells were washed once with PBS then treated with 400 μ L ice-cold lysis buffer (20 mM Tris-HCl pH 7.5, 150 mM NaCl, 1 mM Na₂EDTA, 1 mM EGTA, 1% Triton, 2.5 mM sodium pyrophosphate, 2 mM β -glycerophosphate, 1 mM Na₃VO₄, 1 μ g/mL leupeptin, 1 mM phenylmethanesulfonylfluoride) for 5 min at 5°C. The lysate was sonicated for 15 s and then centrifuged for 10 min at 20,000 x g at 5°C. The supernatant was retained. Protein concentrations were determined by Bradford assay (Bio-Rad) using bovine serum albumin (Bio-Rad) to create a standard curve. PARP cleavage was assayed by sandwich ELISA (Cell Signaling Technology) and performed according to the manufacturer's recommendations. 10 μ g total protein was loaded into each well of a microplate coated with anti-cleaved PARP (Asp214) mouse mAb and allowed to incubate overnight at 5

°C. Rabbit anti-PARP mAb was then added, followed by anti-rabbit IgG conjugated to HRP. Triplicate wells were included for each condition, and the data are representative of both experimental replicates. The data are expressed as fold change from the untreated condition, showing the mean and standard deviation of each measurement.

6.4.6. Cell cycle analysis. 800,000 DU145 cells were plated in 10 cm diameter dishes for 24 h before treatment with test compounds for an additional 24h. 10 μ M EdU was added 30 min before harvest. The cells were harvested by trypsinization and combined with the cell culture supernatant before pelleting at 300 x g. Following overnight fixation in 70% ethanol, the cells were rehydrated in 1% BSA/PBS and processed with the Click-it EdU Alexa Fluor 488 Flow Cytometry assay kit (Invitrogen) using half the recommended A488 reagent. After overnight treatment with 0.2 mg/mL RNase A in 1% BSA/PBS, the cells were stained for DNA content with the provided 7-aminoactinomycin D and analyzed on a FACSCalibur (Becton-Dickinson) instrument. The data were analyzed using FlowJo v8.8.2 (TreeStar) and are representative of two trials.

6.4.7. Phospho-specific Western blot. 800,000 DU145 cells were plated in 10-cm diameter dishes for 24 h. before treatment with test compounds for an additional 18 h. Cells were washed once with ice-cold PBS and lysed in 125 μ L TBS-Tx buffer (50 mM Tris-HCl pH 7.4, 150 mM NaCl, 1 mM EDTA, 1% Triton X100) containing fresh 1 mM PMSF, protease inhibitors (Roche), and phosphatase inhibitors. Lysates were vortexed, placed on ice for 20 min., and then clarified by brief sonication and centrifugation at 14,000 rpm for 10 min. The samples were quantified by Bradford assay and denatured by boiling in Laemmli buffer. 25 μ g of total protein was analyzed by SDS-PAGE using a 13% polyacrylamide gel for RPA2 pS4/S8 (~32 kDa), β -actin (~42 kDa), and CHK1 pS345 (~60 kDa). A 15% gel was used for γ H2Ax (~17 kDa) and a 10% gel was used for CHK2 pT68 (~62 kDa). After transfer to the nitrocellulose membrane and blocking with 0.2% Tween, phosphospecific rabbit anti-

human primary antibodies were used to probe CHK1 (Cell Signaling Technologies), CHK2 (Abcam), γ H2Ax (Abcam), and RPA32 pS4/S8 (Bethyl) overnight at 4 °C. The rabbit anti-human β -Actin (Sigma) antibody was used as a loading control. Goat anti-rabbit, near-IR conjugated secondary antibody (Licor) was added and the bands were visualized on an Odyssey infrared imager (Licor). The experiment was conducted in duplicate and the data are representative of both trials.

6.4.8. Single-cell gel electrophoresis. The apparatus and reagent kit were purchased from Trevigen (Gaithersburg, MD). The assay was performed according to the manufacturer's recommendations. Briefly, 800,000 DU145 cells were plated in 10 cm diameter dishes for 24 h before treatment with test compounds for an additional 24 h. The cells were harvested with a rubber policeman, pelleted by centrifugation, and washed once with ice-cold PBS before being suspended in 37 °C low melting-point agarose at 1×10^5 cells/mL. 50 μ L of the suspension was placed on a 37 °C glass slide and allowed to cool for 30 min. The slides were bathed in lysis buffer for 30 min followed by a 30 min treatment with alkaline unwinding buffer (200 mM NaOH, 1 mM EDTA) at 5 °C. The slides were subjected to electrophoresis at 21V in a prechilled apparatus and fresh unwinding buffer for 30 min. The slides were washed twice in dH₂O and once in 70% ethanol, then dried for 30 min at 45 °C. Dried slides were stained with 100 μ L 1X SYBR Green I in 10 mM Tris-HCl pH 7.5 for 30 min at 5 °C, and excess dye was removed by blotting. Slides were dried and stored at room temperature with desiccant. Comets were visualized using a LSM 5 Pascal confocal microscope with a 5x objective (Zeiss) and scored using CometScore image analysis software (TriTek). A random sampling of 40 cells was analyzed for each condition. The data are displayed as the median and 95% confidence value and are representative of two trials.

6.5. References.

1. Dervan, P.B., Poulin-Kerstien, A.T., Fechter, E.J. and Edelson, B.S. (2005) Regulation of gene expression by synthetic DNA-binding ligands. *Top Curr Chem*, **253**, 1-31.
2. White, S., Szewczyk, J.W., Turner, J.M., Baird, E.E. and Dervan, P.B. (1998) Recognition of the four Watson-Crick base pairs in the DNA minor groove by synthetic ligands. *Nature*, **391**, 468-471.
3. Best, T.P., Edelson, B.S., Nickols, N.G. and Dervan, P.B. (2003) Nuclear localization of pyrrole-imidazole polyamide-fluorescein conjugates in cell culture. *Proc Natl Acad Sci U S A*, **100**, 12063-12068.
4. Suto, R.K., Edayathumangalam, R.S., White, C.L., Melander, C., Gottesfeld, J.M., Dervan, P.B. and Luger, K. (2003) Crystal structures of nucleosome core particles in complex with minor groove DNA-binding ligands. *J Mol Biol*, **326**, 371-380.
5. Dudouet, B., Burnett, R., Dickinson, L.A., Wood, M.R., Melander, C., Belitsky, J.M., Edelson, B., Wurtz, N., Briehn, C., Dervan, P.B. *et al.* (2003) Accessibility of nuclear chromatin by DNA binding polyamides. *Chem Biol*, **10**, 859-867.
6. Nguyen-Hackley, D.H., Ramm, E., Taylor, C.M., Joung, J.K., Dervan, P.B. and Pabo, C.O. (2004) Allosteric inhibition of zinc-finger binding in the major groove of DNA by minor-groove binding ligands. *Biochemistry*, **43**, 3880-3890.
7. Gearhart, M.D., Dickinson, L., Ehley, J., Melander, C., Dervan, P.B., Wright, P.E. and Gottesfeld, J.M. (2005) Inhibition of DNA binding by human estrogen-related receptor 2 and estrogen receptor alpha with minor groove binding polyamides. *Biochemistry*, **44**, 4196-4203.
8. Muzikar, K.A., Nickols, N.G. and Dervan, P.B. (2009) Repression of DNA-binding dependent glucocorticoid receptor-mediated gene expression. *Proc Natl Acad Sci U S A*, **106**, 16598-16603.
9. Nickols, N.G., Jacobs, C.S., Farkas, M.E. and Dervan, P.B. (2007) Modulating hypoxia-inducible transcription by disrupting the HIF-1-DNA interface. *ACS Chem Biol*, **2**, 561-571.
10. Nickols, N.G. and Dervan, P.B. (2007) Suppression of androgen receptor-mediated gene expression by a sequence-specific DNA-binding polyamide. *Proc Natl Acad Sci U S A*, **104**, 10418-10423.
11. Olenyuk, B.Z., Zhang, G.J., Klco, J.M., Nickols, N.G., Kaelin, W.G., Jr. and Dervan, P.B. (2004) Inhibition of vascular endothelial growth factor with a sequence-specific hypoxia response element antagonist. *Proc Natl Acad Sci U S A*, **101**, 16768-16773.
12. Lamont, K.R. and Tindall, D.J. (2010) Androgen regulation of gene expression. *Adv Cancer Res*, **107**, 137-162.
13. Nicolaidis, N.C., Galata, Z., Kino, T., Chrousos, G.P. and Charmandari, E. (2010) The human glucocorticoid receptor: molecular basis of biologic function. *Steroids*, **75**, 1-12.
14. Aranda, A. and Pascual, A. (2001) Nuclear hormone receptors and gene expression. *Physiol Rev*, **81**, 1269-1304.
15. Roche, P.J., Hoare, S.A. and Parker, M.G. (1992) A consensus DNA-binding site

- for the androgen receptor. *Mol Endocrinol*, **6**, 2229-2235.
16. Nelson, S.M., Ferguson, L.R. and Denny, W.A. (2007) Non-covalent ligand/DNA interactions: minor groove binding agents. *Mutat Res*, **623**, 24-40.
 17. Breslauer, K.J., Remeta, D.P., Chou, W.Y., Ferrante, R., Curry, J., Zaunczkowski, D., Snyder, J.G. and Marky, L.A. (1987) Enthalpy-entropy compensations in drug-DNA binding studies. *Proc Natl Acad Sci U S A*, **84**, 8922-8926.
 18. Pelton, J.G. and Wemmer, D.E. (1989) Structural characterization of a 2:1 distamycin A.d(CGCAAATTGGC) complex by two-dimensional NMR. *Proc Natl Acad Sci U S A*, **86**, 5723-5727.
 19. Schultz, P.G. and Dervan, P.B. (1984) Distamycin and penta-N-methylpyrrolocarboxamide binding sites on native DNA. A comparison of methidiumpropyl-EDTA-Fe(II) footprinting and DNA affinity cleaving. *J Biomol Struct Dyn*, **1**, 1133-1147.
 20. Beerman, T.A., McHugh, M.M., Sigmund, R., Lown, J.W., Rao, K.E. and Bathini, Y. (1992) Effects of analogs of the DNA minor groove binder Hoechst-33258 on Topoisomerase-II and Topoisomerase-I mediated activities. *Biochim Biophys Acta*, **1131**, 53-61.
 21. Baron, R.M., Lopez-Guzman, S., Riascos, D.F., Macias, A.A., Layne, M.D., Cheng, G., Harris, C., Chung, S.W., Reeves, R., von Andrian, U.H. *et al.* (2010) Distamycin A inhibits HMGA1-binding to the P-selectin promoter and attenuates lung and liver inflammation during murine endotoxemia. *PLoS One*, **5**, e10656.
 22. Zimmer, C., Puschendorf, B., Grunicke, H., Chandra, P. and Venner, H. (1971) Influence of netropsin and distamycin A on the secondary structure and template activity of DNA. *Eur J Biochem*, **21**, 269-278.
 23. Brosh, R.M., Jr., Karow, J.K., White, E.J., Shaw, N.D., Hickson, I.D. and Bohr, V.A. (2000) Potent inhibition of werner and bloom helicases by DNA minor groove binding drugs. *Nucleic Acids Res*, **28**, 2420-2430.
 24. Pezzoni, G., Grandi, M., Biasoli, G., Capolongo, L., Ballinari, D., Giuliani, F.C., Barbieri, B., Pastori, A., Pesenti, E., Mongelli, N. *et al.* (1991) Biological Profile of Fce-24517, a Novel Benzoyl Mustard Analog of Distamycin-A. *Br J Cancer*, **64**, 1047-1050.
 25. Chenoweth, D.M., Harki, D.A., Phillips, J.W., Dose, C. and Dervan, P.B. (2009) Cyclic pyrrole-imidazole polyamides targeted to the androgen response element. *J Am Chem Soc*, **131**, 7182-7188.
 26. Horoszewicz, J.S., Leong, S.S., Kawinski, E., Karr, J.P., Rosenthal, H., Chu, T.M., Mirand, E.A. and Murphy, G.P. (1983) LNCaP model of human prostatic carcinoma. *Cancer Res*, **43**, 1809-1818.
 27. Chen, C.D., Welsbie, D.S., Tran, C., Baek, S.H., Chen, R., Vessella, R., Rosenfeld, M.G. and Sawyers, C.L. (2004) Molecular determinants of resistance to antiandrogen therapy. *Nat Med*, **10**, 33-39.
 28. Alimirah, F., Chen, J., Basrawala, Z., Xin, H. and Choubey, D. (2006) DU-145 and PC-3 human prostate cancer cell lines express androgen receptor: implications for the androgen receptor functions and regulation. *FEBS Lett*, **580**, 2294-2300.
 29. Edelson, B.S., Best, T.P., Olenyuk, B., Nickols, N.G., Doss, R.M., Foister, S., Heckel, A. and Dervan, P.B. (2004) Influence of structural variation on nuclear

- localization of DNA-binding polyamide-fluorophore conjugates. *Nucleic Acids Res*, **32**, 2802-2818.
30. Tewari, M., Quan, L.T., O'Rourke, K., Desnoyers, S., Zeng, Z., Beidler, D.R., Poirier, G.G., Salvesen, G.S. and Dixit, V.M. (1995) Yama/CPP32 beta, a mammalian homolog of CED-3, is a CrmA-inhibitable protease that cleaves the death substrate poly(ADP-ribose) polymerase. *Cell*, **81**, 801-809.
 31. Dai, Y. and Grant, S. (2010) New insights into checkpoint kinase 1 in the DNA damage response signaling network. *Clin Cancer Res*, **16**, 376-383.
 32. Olson, E., Nievera, C.J., Klimovich, V., Fanning, E. and Wu, X. (2006) RPA2 is a direct downstream target for ATR to regulate the S-phase checkpoint. *J Biol Chem*, **281**, 39517-39533.
 33. Gravel, S., Chapman, J.R., Magill, C. and Jackson, S.P. (2008) DNA helicases Sgs1 and BLM promote DNA double-strand break resection. *Genes Dev*, **22**, 2767-2772.
 34. Matsuoka, S., Huang, M. and Elledge, S.J. (1998) Linkage of ATM to cell cycle regulation by the Chk2 protein kinase. *Science*, **282**, 1893-1897.
 35. Matsuoka, S., Rotman, G., Ogawa, A., Shiloh, Y., Tamai, K. and Elledge, S.J. (2000) Ataxia telangiectasia-mutated phosphorylates Chk2 in vivo and in vitro. *Proc Natl Acad Sci U S A*, **97**, 10389-10394.
 36. Rogakou, E.P., Boon, C., Redon, C. and Bonner, W.M. (1999) Megabase chromatin domains involved in DNA double-strand breaks in vivo. *J Cell Biol*, **146**, 905-916.
 37. Yu, J., Mani, R.S., Cao, Q., Brenner, C.J., Cao, X., Wang, X., Wu, L., Li, J., Hu, M., Gong, Y. *et al.* (2010) An integrated network of androgen receptor, polycomb, and TMPRSS2-ERG gene fusions in prostate cancer progression. *Cancer Cell*, **17**, 443-454.
 38. Masiello, D., Cheng, S., Bublely, G.J., Lu, M.L. and Balk, S.P. (2002) Bicalutamide functions as an androgen receptor antagonist by assembly of a transcriptionally inactive receptor. *J Biol Chem*, **277**, 26321-26326.
 39. Lee, E.C., Zhan, P., Schallhom, R., Packman, K. and Tenniswood, M. (2003) Antiandrogen-induced cell death in LNCaP human prostate cancer cells. *Cell Death Differ*, **10**, 761-771.
 40. Panne, D., Maniatis, T. and Harrison, S.C. (2007) An atomic model of the interferon-beta enhanceosome. *Cell*, **129**, 1111-1123.
 41. Wang, X., Nagase, H., Watanabe, T., Nobusue, H., Suzuki, T., Asami, Y., Shinojima, Y., Kawashima, H., Takagi, K., Mishra, R. *et al.* (2010) Inhibition of MMP-9 transcription and suppression of tumor metastasis by pyrrole-imidazole polyamide. *Cancer Sci*, **101**, 759-766.
 42. Matsuoka, S., Ballif, B.A., Smogorzewska, A., McDonald, E.R., 3rd, Hurov, K.E., Luo, J., Bakalarski, C.E., Zhao, Z., Solimini, N., Lerenthal, Y. *et al.* (2007) ATM and ATR substrate analysis reveals extensive protein networks responsive to DNA damage. *Science*, **316**, 1160-1166.
 43. Cortez, D., Glick, G. and Elledge, S.J. (2004) Minichromosome maintenance proteins are direct targets of the ATM and ATR checkpoint kinases. *Proc Natl Acad Sci U S A*, **101**, 10078-10083.

44. Yoo, H.Y., Shevchenko, A. and Dunphy, W.G. (2004) Mcm2 is a direct substrate of ATM and ATR during DNA damage and DNA replication checkpoint responses. *J Biol Chem*, **279**, 53353-53364.
45. Shi, Y., Dodson, G.E., Mukhopadhyay, P.S., Shanware, N.P., Trinh, A.T. and Tibbetts, R.S. (2007) Identification of carboxyl-terminal MCM3 phosphorylation sites using polyreactive phosphospecific antibodies. *J Biol Chem*, **282**, 9236-9243.
46. Larsen, A.K., Escargueil, A.E. and Skladanowski, A. (2003) Catalytic topoisomerase II inhibitors in cancer therapy. *Pharmacol Ther*, **99**, 167-181.
47. Wu, N., Wu, X.W., Agama, K., Pommier, Y., Du, J., Li, D., Gu, L.Q., Huang, Z.S. and An, L.K. (2010) A novel DNA topoisomerase I inhibitor with different mechanism from camptothecin induces G2/M phase cell cycle arrest to K562 cells. *Biochemistry*, **49**, 10131-10136.
48. Aggarwal, M., Sommers, J.A., Shoemaker, R.H. and Brosh, R.M., Jr. (2011) Inhibition of helicase activity by a small molecule impairs Werner syndrome helicase (WRN) function in the cellular response to DNA damage or replication stress. *Proc Natl Acad Sci U S A*, **108**, 1525-1530.
49. Belitsky, J.M., Nguyen, D.H., Wurtz, N.R. and Dervan, P.B. (2002) Solid-phase synthesis of DNA binding polyamides on oxime resin. *Bioorg Med Chem*, **10**, 2767-2774.
50. Vichai, V. and Kirtikara, K. (2006) Sulforhodamine B colorimetric assay for cytotoxicity screening. *Nat Protoc*, **1**, 1112-1116.
51. Ishiyama, M., Shiga, M., Sasamoto, K., Mizoguchi, M. and He, P.G. (1993) A New Sulfonated Tetrazolium Salt That Produces a Highly Water-Soluble Formazan Dye. *Chem Pharm Bull*, **41**, 1118-1122.